![CAMBRIDGE UNIVERSITY PRESS]

Transmission electron microscopy on a case of *Cyclospora cayetanensis* infection from an immune-competent case confirms and extends prior detailed descriptions of its notably small endogenous stage

Jitender P. Dubey[1] (iD), Jon E. Charlesworth[2] and Bobbi S. Pritt[3]

[1]Animal Parasitic Disease Laboratory, United States Department of Agriculture, Agricultural Research Service, Beltsville Agricultural Research Center, Building 1001, BARC-East, Beltsville, MD 20705-2350, USA; [2]Microscopy and Cell Analysis Core, Mayo Clinic, Rochester, MN 55905, USA and [3]Division of Clinical Microbiology, Department of Laboratory Medicine and Pathology, Mayo Clinic, Rochester, MN 55905, USA

Abstract

Although infections with *Cyclospora cayetanensis* are prevalent worldwide, many aspects of this parasite's life cycle remain unknown. Humans are the only known hosts, existing information on its endogenous development has been derived from histological examination of only a few biopsy specimens. In histological sections, its stages are less than $10\,\mu m$, making definitive identification difficult. Here, confirmation of cyclosporiasis in a duodenal biopsy specimen from an 80-year-old man without any recognized immunodeficiency patient is reported. Asexual forms (schizonts) and sexual forms (gamonts) were located within enterocytes, including immature and mature schizonts, an immature male gamont and a female gamont. Merozoites were small ($<5\,\mu m \times 1\,\mu m$) and contained two rhoptries, subterminal nucleus and numerous micronemes and amylopectin granules. These parasite stages were like those recently reported in the gallbladder of an immunocompromised patient, suggesting that the general life-cycle stages are not altered by immunosuppression.

Introduction

Cyclosporiasis is a global gastrointestinal infection caused by the apicomplexan protozoal parasite, *Cyclospora cayetanensis* (Ortega *et al.*, 1994). Several recent papers review the prevalence, clinical symptoms, diagnosis, epidemiology and treatment of cyclosporiasis (Almeria *et al.*, 2019; Giangaspero and Gasser, 2019; Almeria *et al.*, 2020; Hadjilouka and Tsaltas, 2020; Li *et al.*, 2020; Mathison and Pritt, 2021). Unfortunately, many aspects of this parasite's life cycle remain unknown, and existing information on its endogenous development has been derived from histological examination of only a few biopsy specimens (Bendall *et al.*, 1993; Sifuentes-Osornio *et al.*, 1995; Sun *et al.*, 1996; Deluol *et al.*, 1996; Nhieu *et al.*, 1996; Ortega *et al.*, 1997; Connor *et al.*, 1999; Velásquez *et al.*, 2004; Tsang *et al.*, 2013; Rozenova *et al.*, 2021). Although some of these reports include the diagnosis by electron microscopic examination of intestinal biopsies, the description of the various life-cycle stages remains incomplete, and in some cases, is inaccurate (reviewed in Dubey *et al.*, 2020*a*). To our knowledge, there are no reports of full postmortem findings of any cyclosporiasis patients. The most complete information regarding the structure of life-cycle tissue stages is from a profoundly immunocompromised Honduran man with acquired immunodeficiency syndrome (Dubey *et al.*, 2020*a*). In this extensive morphologic study, the entire gallbladder had been surgically removed and thus allowed for examination of multiple tissue sections by transmission electron microscopy (TEM) (Dubey *et al.*, 2020*a*). There was profuse multiplication of schizonts, and Type II long merozoites were not found. Additionally, sexual stages were described in detail (Dubey *et al.*, 2020*a*). Despite these interesting findings, the authors recognized the limitations of this study in that the stages were from a gallbladder rather than the more common site of infection (intestine) and that the patient was profoundly immunocompromised. Considering these limitations, we report here the diagnosis of clinical cyclosporiasis in an elderly patient by TEM examination of a formalin-fixed, small intestinal biopsy (Velásquez *et al.*, 2004).

For the benefit of uninformed readers, a brief introduction is provided to elucidate the coccidian endogenous life cycle. Following ingestion of sporulated oocysts in contaminated food or water, sporozoites are believed (based on analogy to more detailed data from various species of *Eimeria*) to excyst in the gut lumen and multiply, asexually, in intestinal epithelial cells (Dubey *et al.*, 2020*b*). A few sporozoites may also invade the epithelium of the bile ducts and gallbladder. Based on histological examination of endoscopic biopsies of duodenum or upper jejunum of Peruvian patients, asexual stages were observed within intestinal epithelial cells (presumably enterocytes) (Ortega *et al.*, 1997). Only a few parasites were observed,

and thus results were pioneering but preliminary. These stages were termed Types I and II meronts (Ortega *et al.*, 1997). Type I meronts each contained 8–12 small (3–4 μm long) merozoites; Type II meronts each contained 4 (12–15 μm long) merozoites (Ortega *et al.*, 1997). However, the size of these merozoites was not confirmed by others (reviewed in Dubey *et al.*, 2020*a*). The mode of division was not described.

In the gallbladder of the immunocompromised Honduran man, *C. cayetanensis* stages were found only in epithelial cells, located in a parasitophorous vacuole in the apical aspect of the host cell cytoplasm (Dubey *et al.*, 2020*a*). Mature schizonts were 7.6 × 5.1 μm and contained up to 10 merozoites. The size of merozoites could not be determined by histopathological examination but appeared to be less than 6 μm long. By TEM examination, evidence of schizont division by schizogony was observed (where the parasite nucleus divided into five or more nuclei before segregating into distinct merozoites). A residual body was present in some schizonts, but not in others. The number of generations of schizonts could not be determined because of the profound state of hyper-infection in this host. By light microscopy, individual merozoites and schizonts (containing merozoites) in different phases of development appeared within the same host cell or in adjacent host cells. Whether the course of schizont development in this case was influenced by the immunocompromised status of the patient could not be ascertained.

Materials and methods

Patient's information

The intestinal biopsy evaluated in this study was obtained from an 80-year-old man with type 2 diabetes, chronic kidney disease, hypertension and deafness. He had no known immunosuppressive condition. The full case result and findings from histopathologic examination of small intestinal biopsies was reported by Velásquez *et al.* (2004).

Electron microscopic examination

Tissue was excised from a formalin-fixed paraffin-embedded block, cut to 1 mm cubed pieces and placed in a small nylon specimen bag. The specimen bag was immersed in warmed xylene and placed in a 60°C oven for 90 min and then transferred to absolute ethanol for 30 min at 60°C. The tissue was then subjected stepwise to decreasing concentrations of ethanol to 60% where it is then placed into McDowell's and Trump's fixative (McDowell and Trump, 1976) overnight at 4°C. Following two rinses in 0.1 M sodium phosphate buffer (pH 7.2), the samples were immersed in 1% osmium tetroxide for 1 h at room temperature. Following three washes in distilled water, the samples were placed in 2% aqueous uranyl acetate for 30 min and then rinsed twice in distilled water. The samples were dehydrated in an ethanolic series culminating in two changes of 100% acetone. Tissues were then transferred to a mixture of Spurr's resin (1969) and acetone (1:1) for 30 min, followed by 2 h in 100% resin with two changes. Samples were then placed in fresh 100% Spurr resin in moulds and polymerized at 65°C for 12 h or longer. Semi-thin (0.5 μm) survey sections were cut, placed on glass slides and stained with 1% toluidine blue-O in 1% sodium borate. Ultrathin (90 nm) sections were placed onto copper grids, stained with lead citrate and examined with a JEOL 1400 transmission electron microscope (JEOL, Ltd., Tokyo, Japan) operating at 80 keV.

Results

As noted in prior reports, both asexual and sexual stages were found within parasitophorous vacuoles in the apical portion of the host cell cytoplasm, above the nucleus (Fig. 1). All stages were present within enterocytes, except one that was in a goblet cell (Fig. 2). All parasite forms were smaller than 7 μm. Asexual stages included both immature and mature schizonts. The earliest stage recognized was an uninucleate zoite with a large nucleus, prominent nucleolus and with a few peripheral micronemes (Fig. 3). This stage is akin to an eimerian trophozoite (Dubey
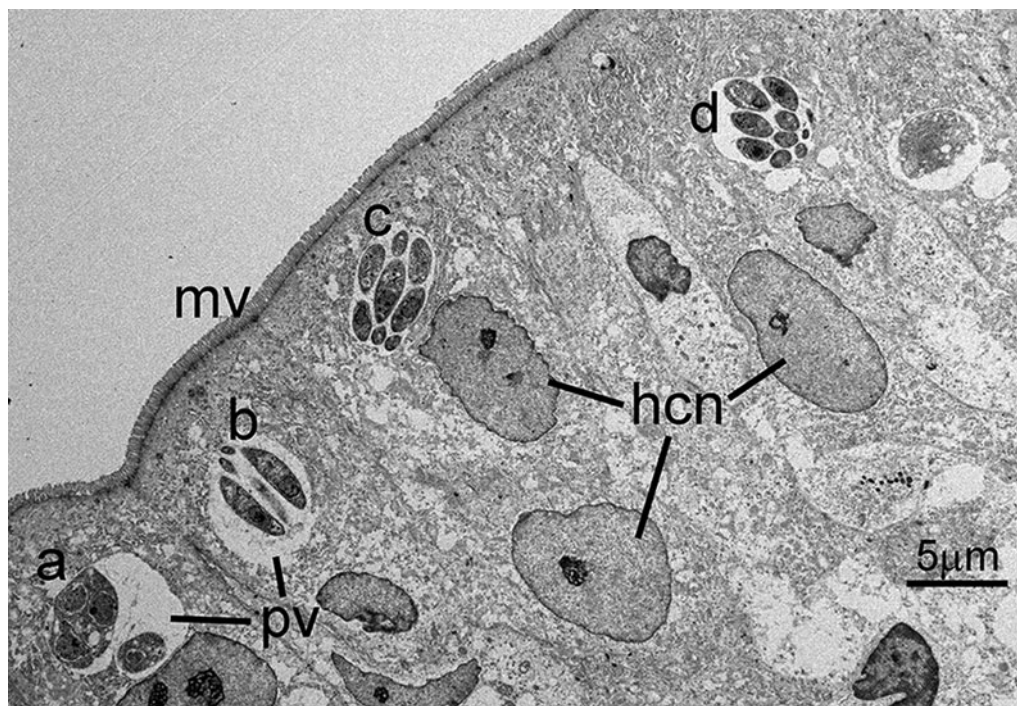

Fig. 1. Transmission electron micrograph of *C. cayetanensis* tissue stages in a duodenal biopsy. Tissue stages (a–d) are located within cytoplasmic parasitophorous vacuoles (pv) at the apical end of infected enterocytes. Note the intact overlying microvillous border (mv) and host cell nuclei (hcn). Four schizonts (a–d) are visible in this section; the schizont in (a) is immature, while the schizonts in (b–d) are mature and contain fully formed merozoites. Note the small size (∼5 μm) of the schizonts.
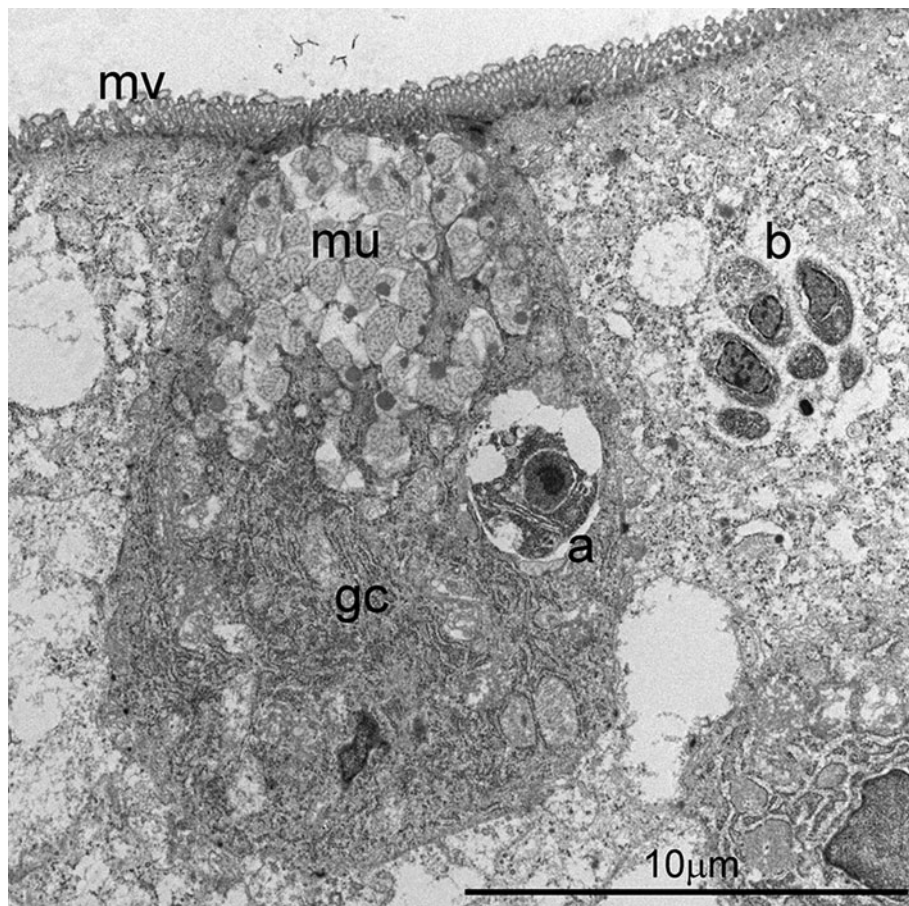
Fig. 2. Transmission electron micrograph of *C. cayetanensis* tissue stages in a duodenal biopsy. A uninucleate parasite (a) is located in a goblet cell (gc) that contains mucin (mu) and profuse endoplasmic reticulin in the basilar region. Note a mature schizont (b) in an adjacent cell. The overlying microvillus (mv) border is intact.
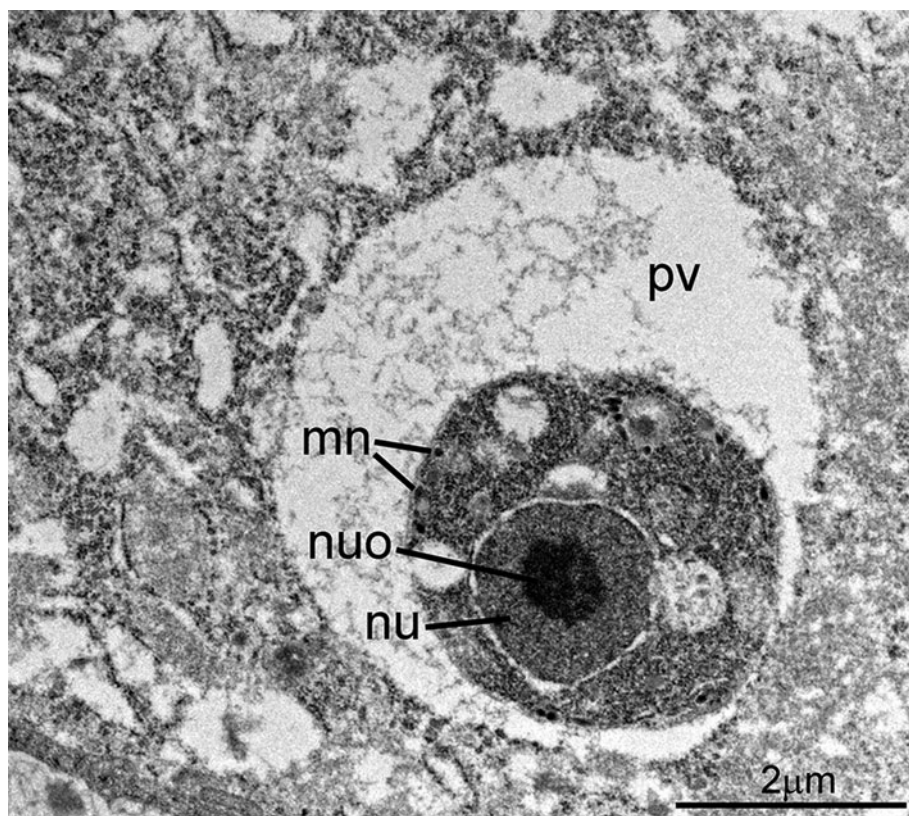

Fig. 3. Transmission electron micrograph of *C. cayetanensis* in a duodenal biopsy. A uninucleate stage is located within a parasitophorous vacuole (pv). Note the large nucleus (nu) with a prominent nucleolus (nuo) and a few micronemes (mn). Other organelles are not present. This stage is like a coccidian trophozoite.
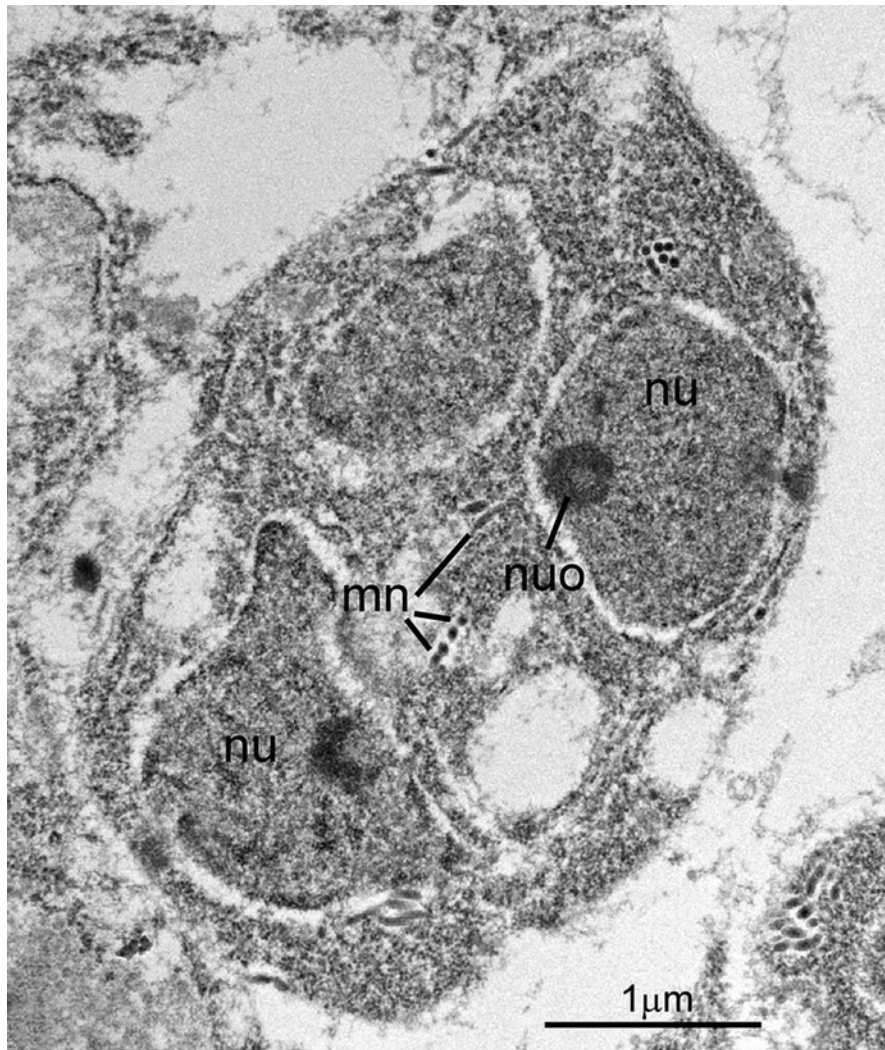
Fig. 4. Transmission electron micrograph showing higher magnification of the *C. cayetanensis* immature schizont shown in Fig. 1. This pear-shaped schizont contains at least two nuclei (nu), each with a nucleolus (nuo). A few micronemes (mi) are seen in cross- and longitudinal sections.
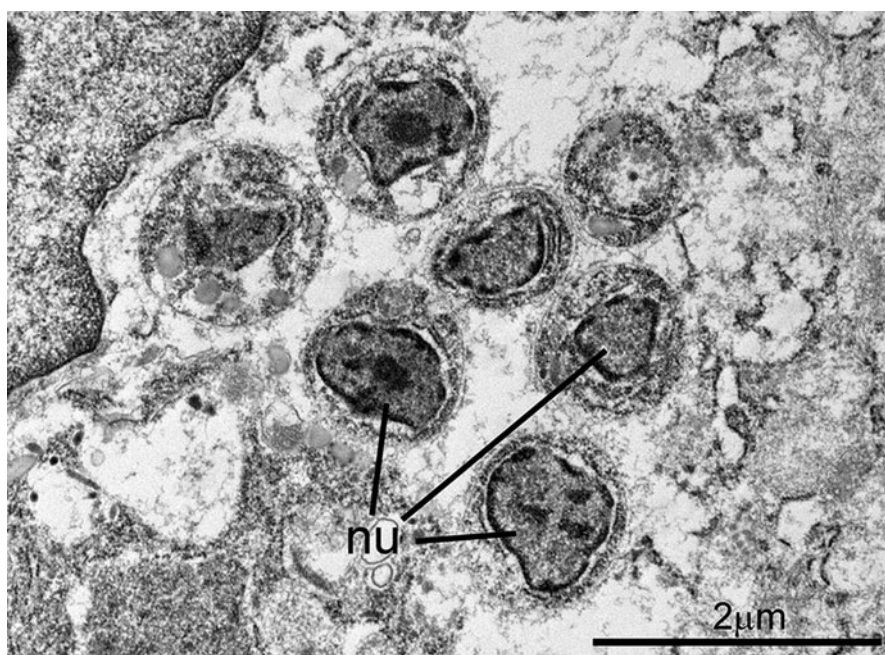

Fig. 5. Transmission electron micrograph of a *C. cayetanensis* mature schizont in a duodenal biopsy. At least six merozoites are cut at the level of the nuclei (nu). There is a seventh possible merozoite, but it is not cut at the level of the nucleus, and thus cannot be confirmed.
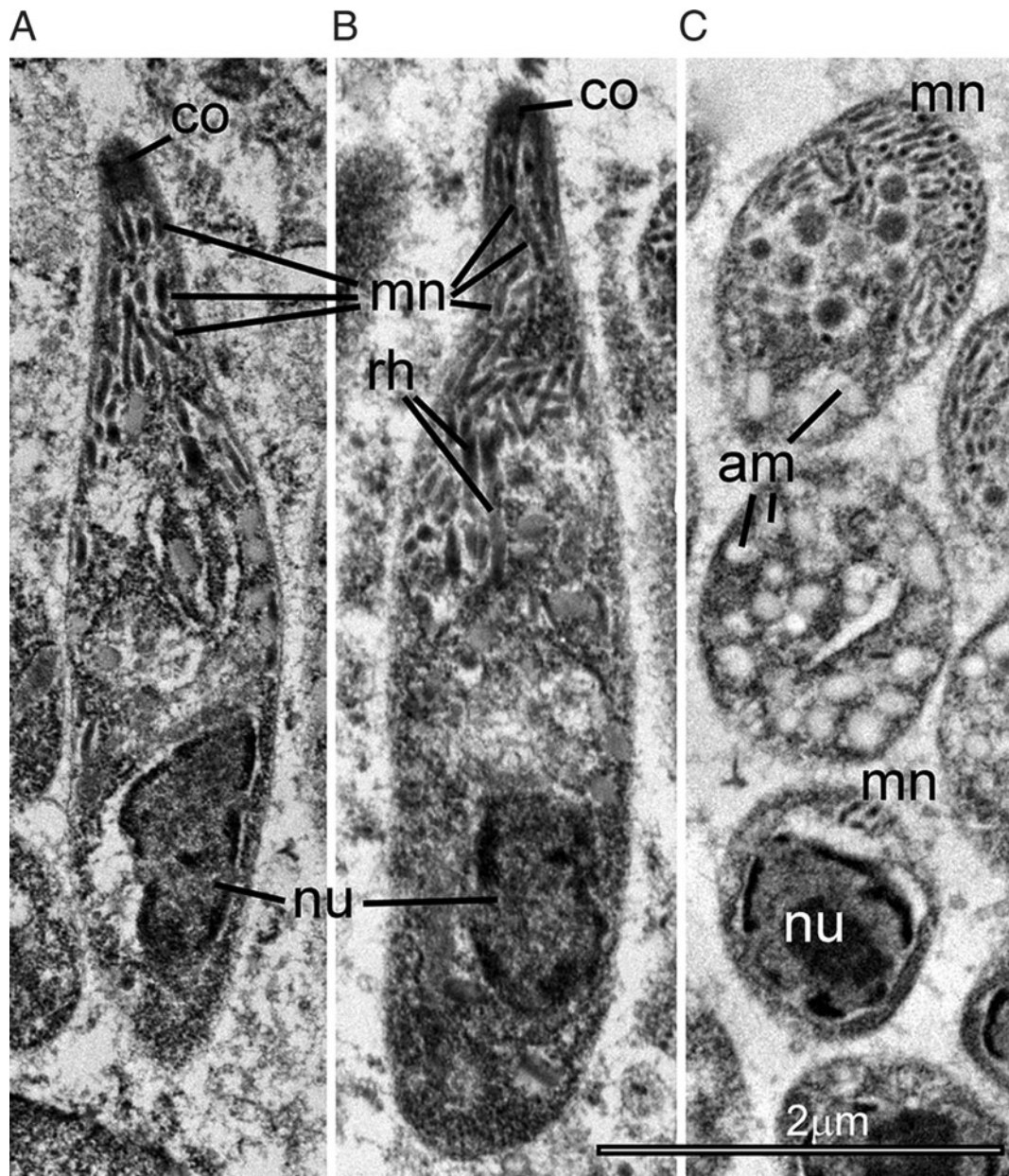
Fig. 6. Transmission electron micrograph of *C. cayetanensis* mature merozoites in a duodenal biopsy. There are two longitudinally cut merozoites (A, B) and several merozoites in oblique section (C). Note the conoid (co) and numerous micronemes (mn) that are concentrated at the conoidal end but are present up to the level of the nucleus. Also note one or two rhoptries (rh), reaching up to the middle of the merozoites. The nucleus (nu) is located sub-terminally. Note only a few amylopectin (am) granules are seen in the two longitudinally cut merozoites, but numerous amylopectin granules are easily visible within the merozoites cut in an oblique section.

et al., 2020*b*). It could not be ascertained if this stage was an early schizont or a gamont. An immature schizont is shown in Fig. 4. This schizont has at least two visible nuclei and several micronemes. There were at least six merozoites in mature schizonts based on the presence of nuclei in each (Fig. 5). A clear-cut residual body was not evident in this example. Figure 6 shows three or more merozoites, with numerous amylopectin granules and micronemes. The micronemes resembled rice grains, less than 250 nm in length; they were concentrated at the conoidal part but a few were seen at the level of the nucleus. The rhoptries were electron dense and no more than two were seen in any merozoite; their blind end reached up to the middle of merozoite length. The nucleus was located subterminally. Two (one immature and one mature) microgamonts were also identified in TEM sections. The immature microgamont contained four peripherally located nuclei, with peripherally arranged chromatin (Fig. 7). The mature microgamont measured $6.2 \times 5.0\,\mu$m and

contained a large residual body and peripherally located microgametes with flagella (Fig. 8). Two macrogamonts ($5 \times 5\,\mu$m, Fig. 9) and $6.5 \times 4.1\,\mu$m (Fig. 10) were also seen. Each macrogamont contained a large nucleus, numerous amylopectin and two types of wall-forming bodies (wfb); wfb1 are larger and less electron dense than the wfb2, which are electron dense. Oocysts were not detected in the sections examined in this case.

Discussion

The asexual and sexual stages in the duodenal biopsy of the present case were essentially like those from the gallbladder of the immunosuppressed patient reported previously (Dubey *et al.*, 2020*a*). Because of the limited size of the intestinal biopsy, TEM examinations were limited to few (<5) infected intestinal villi. Despite the limited size and prior fixation in formalin, both asexual and sexual stages within enterocytes could be
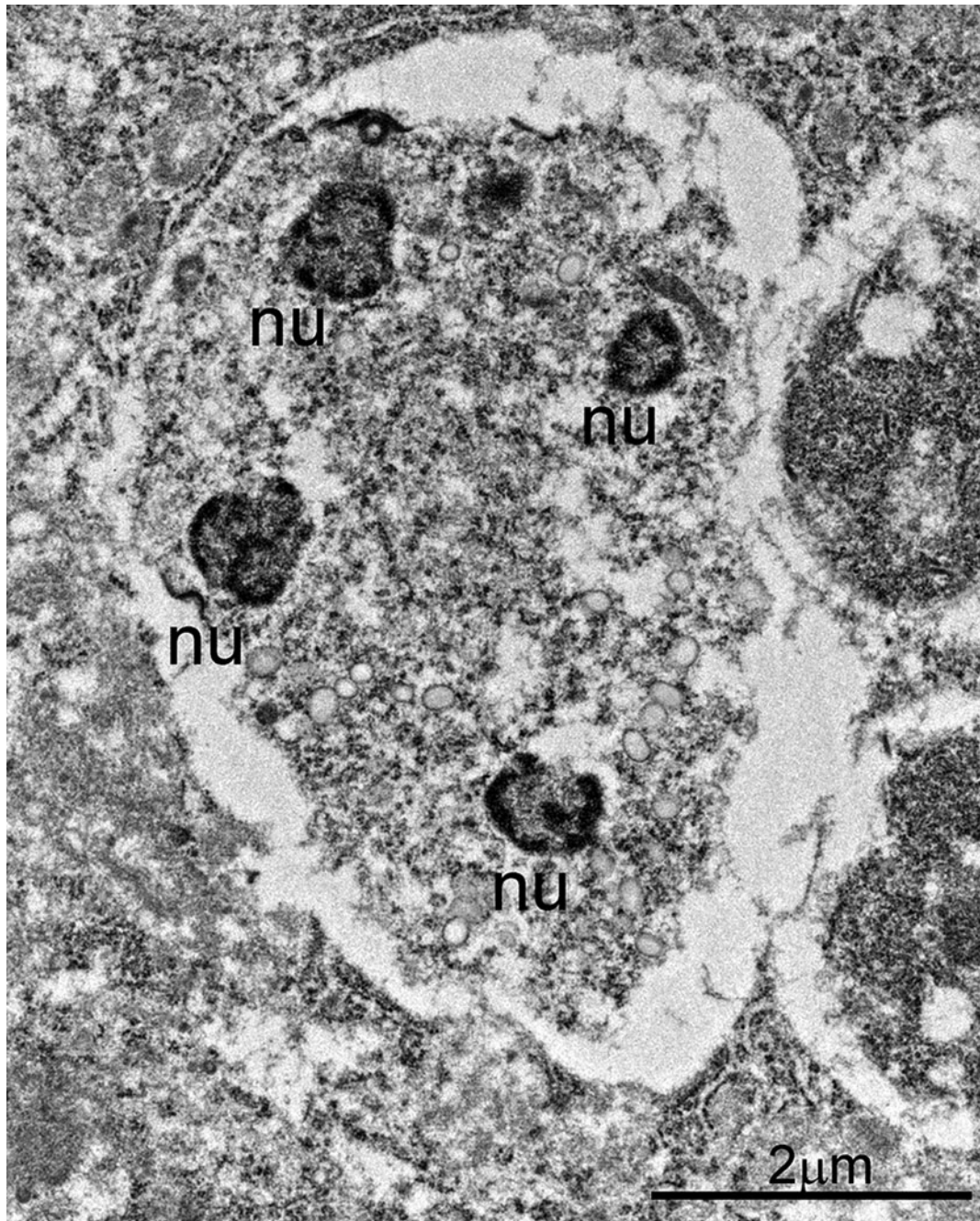
Fig. 7. Transmission electron micrograph of a *C. cayetanensis* immature microgamont (male) in a duodenal biopsy. Note the presence of four peripherally located nuclei (nu) with peripherally located chromatin.

recognized. A uninucleate form within a goblet cell was also noted; to our knowledge, this is the first report of *C. cayetanensis* parasitizing a goblet cell.

Asexual forms observed in this study included both immature and mature schizonts. While it is difficult to differentiate immature schizonts from immature microgamonts by light microscopy, the location of chromatin as visualized by TEM aids in the identification and differentiation of these stages. Specifically, the chromatin is often located at the periphery of the nucleus in multinucleated microgamonts, whereas the chromatin is often compact and not in a peripheral location in multinucleated schizonts.

In the present study, only small-sized schizonts were found and they contained fewer than eight merozoites with variable numbers of amylopectin granules. In general, coccidian merozoites contain only a few amylopectin granules that stain red with periodic acid Schiff reaction. However, in the present case numerous amylopectin

granules were noticed in some merozoites. This is in keeping with the prior report of *C. cayetanensis* involving the gallbladder in an immunocompromised man, where some merozoites contained many amylopectin granules, and others contained only a few (Dubey *et al.*, 2020*a*). Whether these differences are related to generations of merozoites remain unknown. In histological sections, the size and number of merozoites within a schizont can be difficult to determine, unless the merozoites are cut longitudinally (showing both the conoid and the posterior tip and when the nucleus is visible. In the present study, one longitudinally sectioned merozoite (Fig. 6B) was $5.5 \times 1.1 \, \mu m$ long and a maximum of six nuclei could be ascertained in schizonts. This compares with previous results that suggest that *C. cayetanensis* merozoites are tiny (<6 μm). The 12–15 μm long merozoites reported by Ortega *et al.* (1997) were not found in this case or in reports by other authors (reviewed in Dubey *et al.*, 2020*a*). As stated earlier, there are no
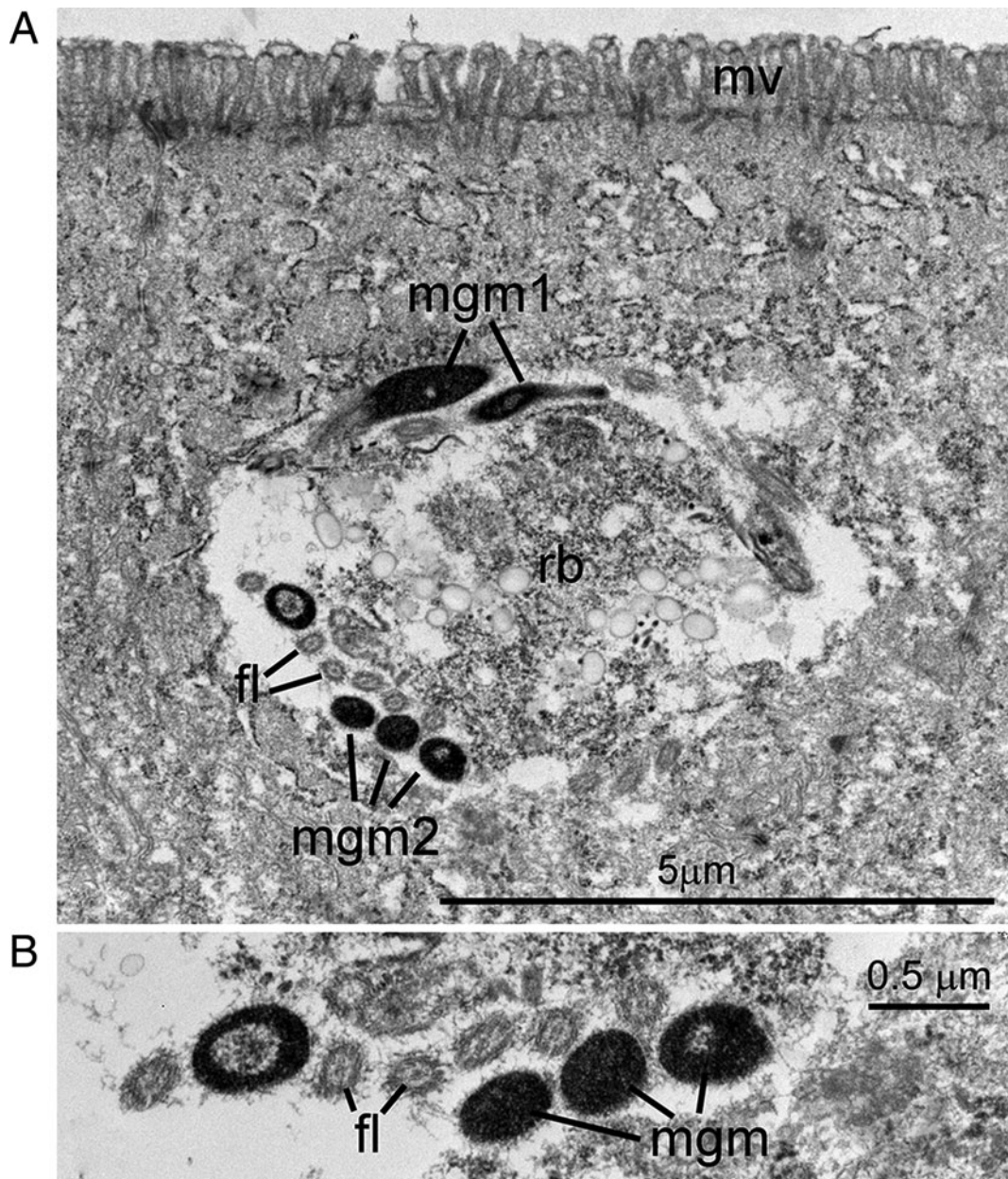
Fig. 8. Transmission electron micrograph of a *C. cayetanensis* mature microgamont (male) in a duodenal biopsy. The microgamont is within a parasitophorous vacuole in the apical aspect of the cell, near the overlying microvillous (mv) brush border. (A) The microgamont contains a large central residual body (rb) and peripherally located flagellated microgametes seen in longitudinal (mgm1) and cross-sections (mgm2). (B) Higher magnification of microgametes with electron-dense nuclei and electron-lucent flagella (fl). Note the cross-section of microtubules in each flagellum.

archived specimens for verification from Ortega's report, and unfortunately there was no scale bars in the published images for evaluation of size (Ortega *et al.*, 1997).

Sexual forms observed in this study included both micro- and macrogamonts. We were able to confirm the presence of flagella in the microgametes within a microgamont (male gamont) as previously described from the gallbladder of a HIV patient (Dubey *et al.*, 2020*a*). Dimensions of microgametes and the number of flagella were not determined. In several apicomplexan parasites, the microgametes have two flagella and sometimes a rudimentary third flagellum (Dubey *et al.*, 2020*b*). In the related coccidian, *Toxoplasma gondii*, the microgametes have a large nucleus (~5 μm long) and flagella that are two to three times longer than the nucleus (Dubey, 2022). We also noted several characteristic wall-forming bodies in the macrogamont (female gamont). The wall-forming bodies disappear when the oocysts are fully formed. In the present case, oocysts were not found in

biopsy sections. However, the patient's stool was positive for *C. cayetanensis* DNA by multiplex PCR panel.

To date, all information on the TEM tissue stages of *C. cayetanensis* has been based on examination of tissues that were initially fixed in formalin. While this has produced satisfactory morphology, it would be advisable to use an optimal fixative for electron microscopy such as glutaraldehyde. Karnovsky fixative (a mixture of formalin and glutaraldehyde) can be used both for light microscopy and TEM. In addition to histologic and TEM examinations, it would also be helpful to visualize parasites on cytological smears to better establish the dimensions of the various parasite forms.

In summary, we confirm the *C. cayetanensis* tissue forms as previously described in the gallbladder of a profoundly immunocompromised man with AIDS, and present, for the first time, evidence of goblet cell infection. These findings contribute to our knowledge of this enigmatic human protozoan parasite.
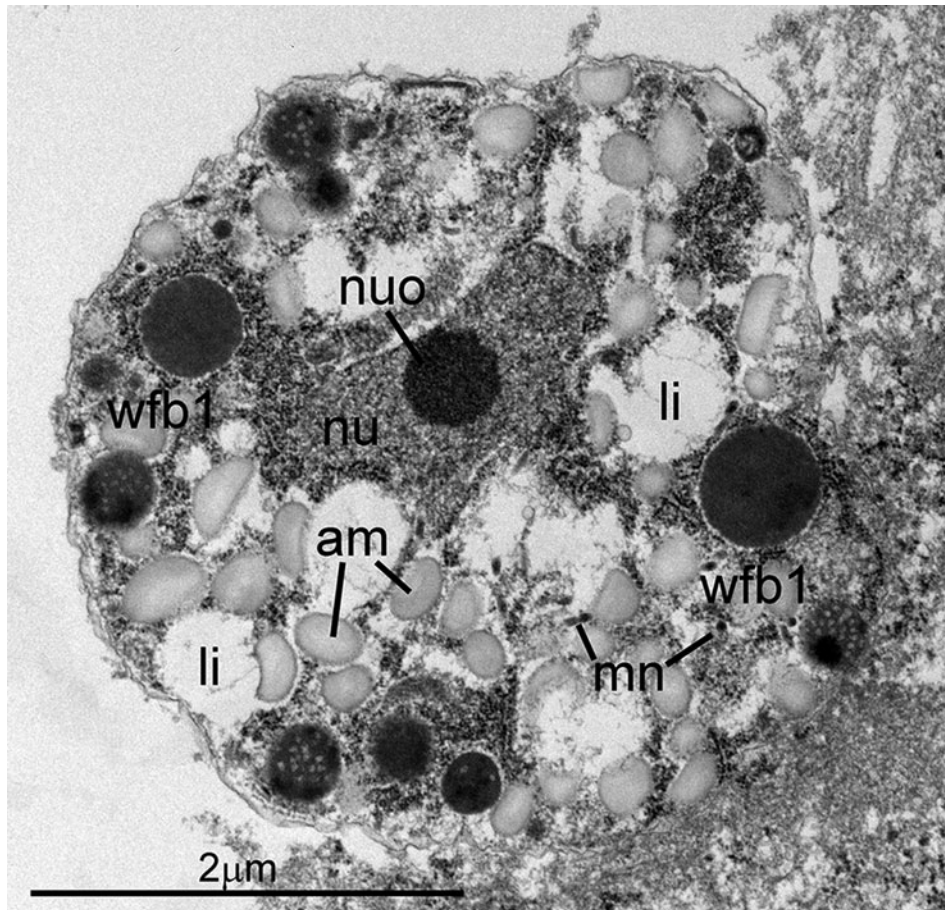
Fig. 9. Transmission electron micrograph of a *C. cayetanensis* macrogamont (female) in a duodenal biopsy. This $5 \times 5\,\mu$m macrogamont contains an elongated nucleus (nu) with a prominent nucleolus (nuo), numerous amylopectin granules (am) and a few lipid bodies (li). Also note peripheral wall-forming bodies (wfb1).
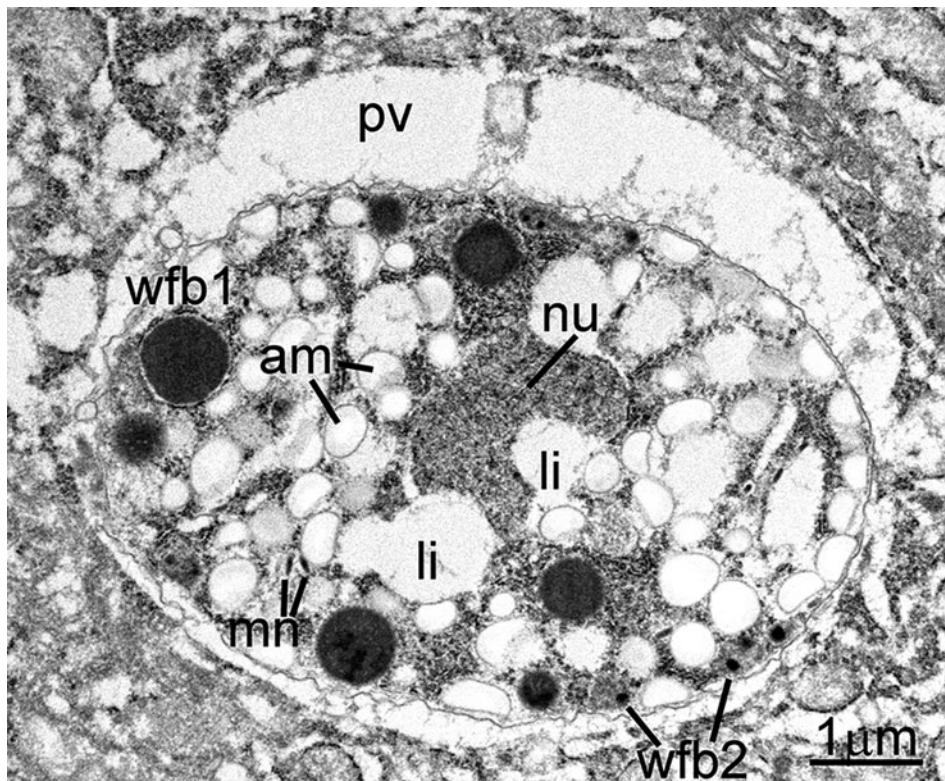

Fig. 10. Transmission electron micrograph of a *C. cayetanensis* macrogamont (female) within a parasitophorous vacuole (pv) in a duodenal biopsy. This 6.8×4.8 μm macrogamont is at a more advanced stage than the macrogamont shown in Fig. 9. Note an elongated nucleus (nu), numerous amylopectin granules (am), few lipid bodies (li) and peripheral wall-forming bodies (wfb1 and wfb2).

References

Almeria S, Cinar HN and Dubey JP (2019) *Cyclospora cayetanensis* and cyclosporiasis: an update. *Microorganisms* **7**, 317.

Almeria S, Cinar HN and Dubey JP (2020) In Dubey JP (ed). *Coccidiosis in Livestock, Poultry, Companion Animals, and Humans*. Boca Raton, Florida, USA: CRC Press, pp. 268–312.

Bendall RP, Lucas S, Moody A, Tovey G and Chiodini PL (1993) Diarrhoea associated with cyanobacterium-like bodies: a new coccidian enteritis of man. *Lancet* **341**, 590–592.

Connor BA, Reidy J and Soave R (1999) Cyclosporiasis: clinical and histopathologic correlates. *Clinical Infectious Diseases* **28**, 1216–1222.

Deluol AM, Teilhac MF, Poirot JL, Heyer F, Beaugerie L and Chatelet FP (1996) *Cyclospora* sp: life cycle studies in patient by electron microscopy. *Journal of Eukaryotic Microbiology* **43**, 128S–129S.

Dubey JP (2022) *Toxoplasmosis of Animals and Humans*, 3rd Edn. Boca Raton, Florida, USA: CRC Press.

Dubey JP, Almería S, Mowery JD and Fortes J (2020a) Endogenous developmental cycle of the human coccidian *Cyclospora cayetanensis*. *Journal of Parasitology* **106**, 295–307.

Dubey JP, Lindsay DS, Jenkins MC and Bauer C (2020b) Biology of intestinal coccidia. In Dubey JP (ed). *Coccidiosis in Livestock, Poultry, Companion Animals, and Humans*. Boca Raton, Florida, USA: CRC Press, pp. 1–36.

Giangaspero A and Gasser RB (2019) Human cyclosporiasis. *The Lancet. Infectious Diseases* **19**, e226–e236.

Hadjilouka A and Tsaltas D (2020) *Cyclospora cayetanensis* – Major outbreaks from ready to eat fresh fruits and vegetables. *Foods (Basel, Switzerland)* **9**, 1703.

Li J, Cui Z, Qi M and Zhang L (2020) Advances in cyclosporiasis diagnosis and therapeutic intervention. *Frontiers in Cellular and Infection Microbiology* **10**, 43.

Mathison BA and Pritt BS (2021) Cyclosporiasis – updates on clinical presentation, pathology, clinical diagnosis, and treatment. *Microorganisms* **9**, 1863.

McDowell EM and Trump BF (1976) Histologic fixatives suitable for diagnostic light and electron microscopy. *Archives of Pathology and Laboratory Medicine* **100**, 405–414.

Nhieu JTV, Nin F, Fleury-Feith J, Chaumette MT, Schaeffer A and Bretagne S (1996) Identification of intracellular stages of *Cyclospora* species by light microscopy of thick sections using hematoxylin. *Human Pathology* **27**, 1107–1109.

Ortega YR, Gilman RH and Sterling CR (1994) A new coccidian parasite (Apicomplexa: Eimeriidae) from humans. *Journal of Parasitology* **80**, 625–629.

Ortega YR, Nagle R, Gilman RH, Watanabe J, Miyagui J, Quispe H, Kanagusuku P, Roxas C and Sterling CR (1997) Pathologic and clinical findings in patients with cyclosporiasis and a description of intracellular parasite life-cycle stages. *Journal of Infectious Diseases* **176**, 1584–1589.

Rozenova K, Pritt BS and Said S (2021) Uncommom cause of emesis and diarrhea in a nonverbal elderly patient. *Gastroenterology* **160**, e5–e7.

Sifuentes-Osornio J, Porras-Cortés G, Bendall RP, Morales-Villarreal F, Reyes-Terán G and Ruiz-Palacios GM (1995) *Cyclospora cayetanensis* infection in patients with and without AIDS: biliary disease as another clinical manifestation. *Clinical Infectious Diseases* **21**, 1092–1097.

Spurr AR (1969) A low-viscosity epoxy resin embedding medium for electron microscopy. *Journal of Ultrastructure Research* **26**, 31–43.

Sun T, Ilardi CF, Asnis D, Bresciani AR, Goldenberg S, Roberts B and Teichberg S (1996) Light and electron microscopic identification of *Cyclospora* species in the small intestine. Evidence of the presence of asexual life cycle in human host. *American Journal of Clinical Pathology* **105**, 216–220.

Tsang OTY, Wong RWC, Lam BHS, Chan JMC, Tsang KY and Leung WS (2013) *Cyclospora* infection in a young woman with human immunodeficiency virus in Hong Kong: a case report. *BMC Research Notes* **6**, 521.

Velásquez JN, Carnevale S, Cabrera M, Kuo L, Chertcoff A, Mariano M, Bozzini JP, Etchart C, Argento R and Di Risio C (2004) *Cyclospora cayetanensis* en pacientes con SIDA y diarrea crónica. *Acta Gastroenterologica Latinoamericana* **34**, 133–137.